PHYSICAL REVIEW E, VOLUME 63, 045301(R)

Flow pattern dynamics in convecting liquid helium

R. G. Matley,[1] W. Y. T. Wong,[1] M. S. Thurlow,[1] P. G. J. Lucas,[1,*] M. J. Lees,[1] O. J. Griffiths,[1] and A. L. Woodcraft[2]
[1]*Department of Physics and Astronomy, University of Manchester, Manchester M13 9PL, United Kingdom*
[2]*Department of Physics, Queen Mary & Westfield College, University of London, London E1 4NS, United Kingdom*
(Received 20 June 2000; published 20 March 2001)

We present experimental data which correlate thermal measurements and flow visualization in convecting liquid ^{4}He. For a small range $R_C<R<R_1$ of the Rayleigh number R above the convection threshold value R_C a robust stationary pattern is observed. This pattern exhibits periodic pulsation when $R>R_1$, generating thermal oscillations as in earlier reports. At higher R values the time dependence becomes aperiodic with the surprising appearance of spiral-defect chaos at an aspect ratio smaller than has previously been reported.

DOI: 10.1103/PhysRevE.63.045301 PACS number(s): 47.54.+r, 47.20.Bp, 47.27.Te

INTRODUCTION

Rayleigh-Bénard convection occupies a central role in the physics of pattern formation and the study of nonlinear phenomena [1]. Above the conduction-convection threshold it is relatively straightforward experimentally to control the magnitude of the nonlinear terms in the fluid dynamical equations by adjusting the Rayleigh number R. Advances in image-processing technology coupled with the experimental technique of shadowgraphy [2] permit the viewing of the two-dimensional convection flow pattern close to the threshold in room temperature fluids. In addition, the mechanisms behind the various instabilities of the convection roll pattern of an infinite layer in the weakly nonlinear regime above the threshold are well understood [3].

In recent years research has focused on fluids with Prandtl number $\sigma \lesssim 1$ because time-dependent states arise [3] at Rayleigh numbers close to the threshold value R_C, allowing the study of spatiotemporal chaotic states [4] in the weakly nonlinear regime. In this connection the compressed gases argon [5] and CO_2 [6] with $\sigma \sim 1$, have proven to be very useful in identifying flow pattern phenomena such as the target instability [7] and spiral-defect chaos [8], as well as in verifying the results of the calculations of Busse and Clever [3].

Liquid ^{4}He, with a minimum σ of about 0.5, is also useful with several important advantages over compressed gases: its heat capacity is large compared with the cell containing walls, the resolution of thermometry at cryogenic temperatures can be very high, and the ratio of the heat passing through the fluid to that passing though the sidewalls is much higher. These features facilitated the discovery in the 1980s by Ahlers *et al.* [9] of periodic states which appeared as thermal oscillations with frequency and amplitude dependent on $\epsilon=(R-R_C)/R_C$ in the range $0.09<\epsilon<0.2$. The mechanism driving such oscillatory states has never been understood, in part because of the lack of flow visualization at cryogenic temperatures at that time. In this Rapid Communication we report observations of the time series of these periodic states in liquid helium and connect them with simultaneous observations of the spatiotemporal behavior of the flow pattern using our cryogenic shadowgraphy apparatus [10,11]. Data are also presented on patterns showing spatiotemporal chaos at higher values of ϵ, including spiral-defect chaos.

EXPERIMENT

A detailed description of the experimental equipment exists already [10], together with an improved version [11]. The experimental cell is an upright cylindrical volume of radius 10.0 ± 0.1 mm and height [12] 0.61 ± 0.04 mm so that the aspect ratio $\Gamma=16.4$. The upper horizontal boundary is a sapphire window thermally clamped to a copper platform maintained at a fixed temperature $T_U=2.980$ K. The lower boundary is of chromium-plated copper thermally isolated from the surroundings and includes a heater for supplying the vertical heat current. It is useful to define the parameter $\epsilon_p=(P-P_C)/P_C$, where P is the rate at which heat flows through the fluid layer and P_C its value at the onset of convection. We do this as it is the power, rather than the Rayleigh number, that is under direct experimental control. A matched pair of carbon resistance thermometers mounted on the upper and lower boundaries are wired as two of the arms of an ac resistance bridge. The bridge provides a high resolution measurement (1 in 10^6) of the temperature difference between the two boundaries, and hence of ϵ. The thermally insulating sidewalls are of Vespel SP-22. For the ^{4}He in the cell, the Prandtl number is 0.52, the vertical ($\tau_V=d^2/D_T$) and horizontal ($\tau_H=\Gamma^2\tau_V$) thermal diffusion times are respectively $\tau_V=7.75$ s and $\tau_H=2082$ s, where D_T is the thermal diffusivity of the fluid, and the Boussinesq approximation is satisfied extremely well. The cryogenic shadowgraphy visualization system permits imaging of the flow pattern over the whole of the cell: with the pattern contrast falling off as $\epsilon^{1/2}$, the limit of clear resolution of a pattern occurs at about $\epsilon=0.06$.

RESULTS

The behavior of the flow pattern, which was allowed to develop naturally, falls into several regimes dependent on the value of ϵ. For $0<\epsilon\lesssim\epsilon_1$, where $\epsilon_1=0.06\pm0.03$ ($0<\epsilon_p \lesssim \epsilon_{p1}$, where $\epsilon_{p1}=0.15\pm0.03$), the temperature difference between the two boundaries, as measured by the resistance bridge, shows no time dependence. This is in accordance

*Corresponding author. Email address: Peter.Lucas@man.ac.uk

 ©2001 The American Physical Society

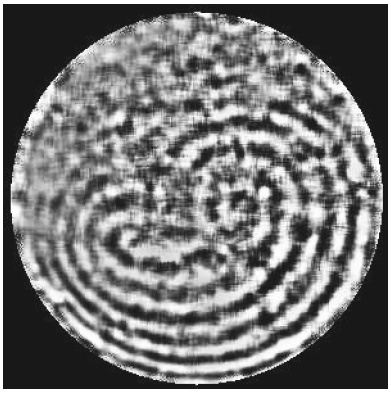

FIG. 1. Time-independent convection state at $\epsilon=0.058$, $\epsilon_p=0.146$. This image is the average of 26 consecutive images taken at 60 s intervals.

with the measurements of Gao and Behringer [13] who obtained $\epsilon_1 \approx 0.09$ for $\Gamma \gtrsim 15$. The errors on ϵ and ϵ_p result almost entirely from uncertainty in obtaining the critical temperature difference and critical power. The flow pattern is shown in Fig. 1. It can be seen that the flow pattern, although based on curved parallel convection rolls, resembles a cardioid in shape. This state was found to be stable for at least $23\tau_H$, as long as we are able to observe with our present apparatus. Time independence was found consistently in this range of ϵ regardless of the history of the heating sequence used to achieve the selected value of ϵ.

In the range $0.06<\epsilon\leqslant 0.07$ ($0.150<\epsilon_p\leqslant 0.161$) the stationary pattern bifurcates to either of two periodic states. When periodic, the time series can be roughly sinusoidal as in Fig. 2, with one major peak in the power spectrum at $\tau=1.5\pm 0.2\tau_H$, or can exhibit oscillations with an additional major peak in the power spectrum usually at twice this period. Periodic states of this kind have been recorded before in convection experiments in liquid helium by several groups as summarized by Behringer [9], and Gao and Behringer [13]. The periodic states observed by us seem to exhibit hysteresis over a very narrow range of ϵ_p, as can be seen in the inset to Fig. 3: this is probably due to critical slowing down at the Hopf bifurcation, but it is possible that the bifurcation is subcritical. To distinguish between the two would require experiments with waiting times not currently possible. It was also observed that in this range of ϵ the convecting state can

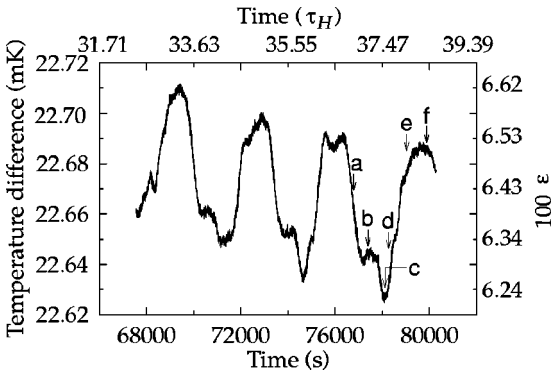

FIG. 2. Time series of temperature difference at $\epsilon_p=0.154$

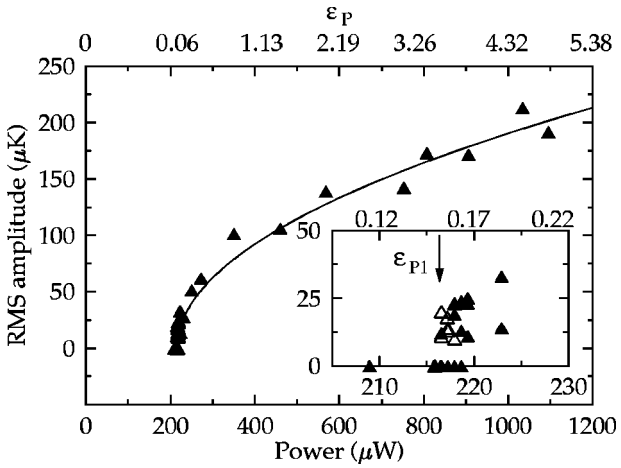

FIG. 3. Growth of the amplitude of temperature difference oscillations with applied power. The solid line is a square root function fitted to the data. The inset shows stationary (zero amplitude) and time-dependent states in a narrow range of power. Closed symbols denote increasing power; open symbols, decreasing power. ϵ_{p1} marks the onset of time dependence.

switch from being stationary to time dependent or vice-versa even after being apparently stable for many τ_H. Periodic time dependence was always observed in the range $0.07<\epsilon\leqslant 0.10$ ($0.161<\epsilon_p\leqslant 0.22$).

In Fig. 4 we show a sequence of images of the flow pattern when the cell is in the convection state with the time-series shown in Fig. 2: images for time-series with more than one major peak in the power spectrum are not available. It can be seen that the pattern changes from one corresponding to the cardioid shape seen in the stationary regime to one in which the rolls unfold into concentric rings after which a dislocation glides in to change the pattern to a single-armed spiral. The spiral then drifts away from the geometric center of the cell, leaving a pattern of slightly curved parallel rolls. Subsequently the curvature increases to reform the cardioid shape, and the whole sequence repeats itself. It is clear that the pattern changes associated with the periodic state are considerably more complicated than a simple change in the number of rolls arising from crossing the skew-varicose instability boundary, as presciently discussed by Gao and Behringer [13]. Although great care was taken in manufacturing the cell to ensure the upper and lower boundaries were parallel, small imperfections may exist which may be responsible for the cardioid shape rather than the set of parallel rolls known to be the base state of the convection onset for compressed gases [5]. Nevertheless, the pattern is robust in that it reappeared after the experiment had been warmed to room temperature and cooled down again.

When $\epsilon\gtrsim 0.15$ ($\epsilon_p\gtrsim 0.33$), periodic variations in the temperature difference give way to aperiodic time dependence with a broad power spectrum. The pattern is now one of slow constant movement of gently curved rolls, sometimes in the form of a giant spiral, with defects present, characteristic of phase or weak turbulence. Further work is planned in the range $0.10\lesssim\epsilon\lesssim 0.15$ ($0.22\lesssim\epsilon_p\lesssim 0.33$) to study the onset of aperiodicity.

The rms amplitude of the oscillations in the aperiodic

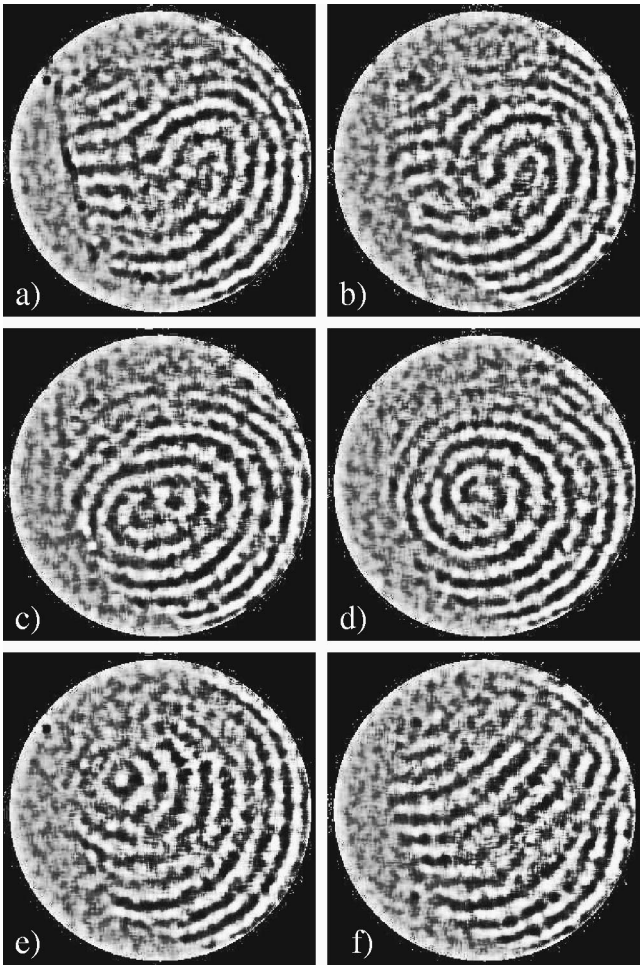

FIG. 4. Images of time-dependent convection. The images were taken at the times marked *a*-*f* in Fig. 2. Blank areas of the image result from saturation of the CCD camera due to slight nonuniformity in the illumination.

state follows approximately a square root dependence on $\epsilon_p - \epsilon_{p1}$, as shown in Fig. 3, and is of the order of 1% of the mean temperature difference across the fluid.

As ϵ increases through the range $0.15 \lesssim \epsilon \lesssim 1.6$ ($0.33 \lesssim \epsilon_p \lesssim 3.8$) the disorder of the pattern increases to a state

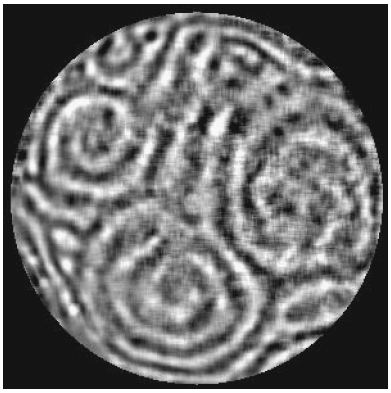

FIG. 5. Convection pattern resembling spiral-defect chaos at $\epsilon = 0.9$, $\epsilon_p = 2.0$.

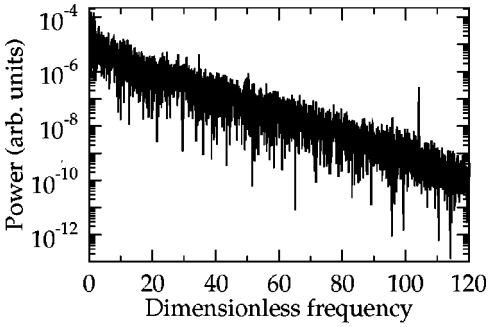

FIG. 6. Power spectrum of the temperature difference oscillations for the state shown in Fig. 5. The oscillation frequency has been scaled by τ_H.

where there are many rapidly changing small features including spirals and targets separated by more continuous lengths of rolls. A typical image is shown in Fig. 5, and is very similar to the state of spiral-defect chaos (SDC) first reported by Morris *et al.* [8]. The fluid parameters in our experiment are within the range of stability of SDC as determined by Liu and Ahlers [14], and our aspect ratio would constitute the lowest value where SDC has been seen. The power spectrum corresponding to the fluid being in this state is shown in Fig. 6: the roll-off is slower than when the fluid is in the aperiodic state at $\epsilon = 0.4$ ($\epsilon_p = 0.9$).

At still higher values of ϵ ($\epsilon \gtrsim 2.6$, $\epsilon_p \gtrsim 6.3$), the rolls have started to develop a wavy appearance along their lengths, but the general pattern is still that of SDC. This is consistent with the crossing of the skew-varicose or oscillatory instability boundaries [3]. The transition to wavy rolls is complete when $\epsilon \gtrsim 5$ ($\epsilon_p \gtrsim 14$). In this range of ϵ, most of the time the wavy rolls adopt a random pattern, but at irregular intervals an expanding target pattern appears for a few tens of τ_V, as shown in Fig. 7. The wavelength distributions for all the ϵ values employed show the distribution becoming broader and the mean of local pattern wavelengths increasing with ϵ, consistent with the calculations of Busse and coworkers [3].

CONCLUSION

In summary, we have for the first time correlated changes in the flow pattern of convecting liquid helium with thermal

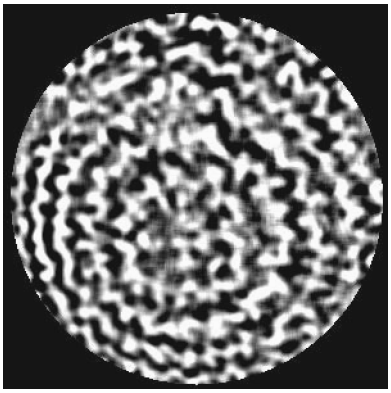

FIG. 7. Wavy convection rolls at $\epsilon = 6.0$, $\epsilon_p = 17.4$ exhibiting an expanding target pattern over a short time scale of order tens of τ_V.

measurements similar to some of the periodic states observed in earlier experiments [9,13]. This information should assist in understanding the origin of this periodicity. We have shown that for a cylindrical cell of aspect ratio 16.4 containing liquid helium with a Prandtl number of 0.52, the flow pattern appearance changes as ϵ passes through a number of distinct regimes including a state which is probably spiral-defect chaos. Our results demonstrate the unique nature of liquid helium as a fluid for convection studies in combining high resolution measurements of mean thermal parameters with observations of the convection pattern.

ACKNOWLEDGMENTS

We gratefully acknowledge support from the EPSRC and a useful discussion with Professor T. Mullin.

[1] M. C. Cross and P. C. Hohenberg, Rev. Mod. Phys. **65**, 851 (1993).

[2] W. Merzkirch, in *Methods of Experimental Physics Volume 18—Fluid Dynamics, Part A*, edited by R. J. Emrich (Academic Press, New York, 1981), p. 345.

[3] F. H. Busse and R. M. Clever, J. Fluid Mech. **91**, 319 (1979).

[4] D. A. Egolf, E. V. Melnikov, W. Pesch, and R. E. Ecke, Nature (London) **404**, 733 (2000).

[5] V. Croquette, Comput. Math. Appl. **30**, 113 (1989); **30**, 153 (1989).

[6] E. Bodenschatz, W. Pesch, and G. Ahlers, Annu. Rev. Fluid Mech. **32**, 709 (2000).

[7] Y. Hu, R. E. Ecke, and G. Ahlers, Phys. Rev. Lett. **72**, 2191 (1994).

[8] S. W. Morris, E. Bodenschatz, D. S. Cannell, and G. Ahlers, Phys. Rev. Lett. **71**, 2026 (1993).

[9] G. Ahlers and R. W. Walden, Phys. Rev. Lett. **44**, 445 (1980); R. P. Behringer, J. N. Shaumeyer, C. A. Clark, and C. C. Agosta, Phys. Rev. A **26**, 3723 (1982); R. W. Walden, *ibid.* **27**, 1255 (1983); R. P. Behringer, Rev. Mod. Phys. **57**, 657 (1985).

[10] A. L. Woodcraft, P. G. J. Lucas, R. G. Matley, and W. Y. T. Wong, J. Low Temp. Phys. **114**, 109 (1999).

[11] P. G. J. Lucas, R. G. Matley, M. S. Thurlow, and W. Y. T. Wong, Physica B **284-288**, 2061 (2000).

[12] R. G. Matley, R. D. Alcock, and P. G. J. Lucas (unpublished).

[13] H. Gao and R. P. Behringer, Phys. Rev. A **30**, 2837 (1984).

[14] J. Liu and G. Ahlers, Phys. Rev. Lett. **77**, 3126 (1996).